GEOPHYSICAL RESEARCH LETTERS, VOL. 33, L17306, doi:10.1029/2006GL027058, 2006



# On the stability of a geodetic no-net-rotation frame and its implication for the International Terrestrial Reference Frame

Corné Kreemer,[1] David A. Lavallée,[2] Geoffrey Blewitt,[1,3] and William E. Holt[4]

Received 1 June 2006; revised 15 July 2006; accepted 31 July 2006; published 7 September 2006.

[1] One of the important implications of a no-net-rotation (NNR) model of the Earth's horizontal surface velocity is that it is used as a constraint in the definition of the International Terrestrial Reference Frame (ITRF). We present here our most recent estimates of an NNR model (GSRM-NNR-2) that uses over 5700 geodetic station velocities. We test the sensitivity of our model by varying data input and model assumptions. The difference between our various models is maximally 0.6 mm $yr^{-1}$, but can be larger if we use only a geographically limited core velocity data set, or if a significant bias in frame origin translation rate exists. Although plate boundary zones should not be considered as being part of rigid plates (Kreemer and Holt, 2001), the details of the velocity field within the plate boundaries have an insignificant effect on the NNR frame. The difference between the various NNR models that we test is small compared to the difference between our NNR models and ITRF2000, which can be up to 3.1 mm $yr^{-1}$. We conclude that the ITRF2000 does not satisfy the NNR condition when considering an NNR model that is based on the actual present-day velocity of the entire Earth's surface, instead of NNR-NUVEL-1A. **Citation:** Kreemer, C., D. A. Lavallée, G. Blewitt, and W. E. Holt (2006), On the stability of a geodetic no-net-rotation frame and its implication for the International Terrestrial Reference Frame, *Geophys. Res. Lett.*, *33*, L17306, doi:10.1029/2006GL027058.

## 1. Introduction

[2] By convention [e.g., *McCarthy and Petit*, 2004], the time evolution of the International Terrestrial Reference Frame (ITRF) is defined such that there should be no-net-rotation (NNR) of the frame with respect to the Earth's lithosphere. In practice the ITRF2000 orientation time evolution was defined by minimizing its 3 rotation rates with respect to the NNR-NUVEL-1A plate motion model using the horizontal velocities of a polyhedron of core ITRF sites [*Altamimi et al.*, 2002, 2003]. The NNR condition is kinematically defined by setting the following integral over the Earth's surface to be zero [*Solomon and Sleep*, 1974]:

$$\oint\int_{surface} [\bar{v} \times \bar{r}] dA = 0 \qquad (1)$$

where $\bar{v}$ is the horizontal velocity at surface position $\bar{r}$, and dA is an infinitesimal element of surface area at $\bar{r}$. In practice we evaluate (1) over finite areas (0.6° by 0.5°). From (1) one can derive an NNR model from any plate motion model. NNR-NUVEL-1A [*Argus and Gordon*, 1991] is one such model that satisfies the NNR condition, but is based on a surface velocity model of the Earth (i.e., NUVEL-1A [*DeMets et al.*, 1994]) that incorrectly describes the present-day velocity of part of the Earth's surface [*Kreemer and Holt*, 2001]. These shortcomings of NNR-NUVEL1A result from the Earth's surface being solely parameterized by rigid spherical caps (thereby ignoring the deforming plate boundary zones, which can be very wide), and from errors in NUVEL-1A's estimate of present-day relative plate motions [e.g., *Sella et al.*, 2002; *Kreemer et al.*, 2003].

[3] The alignment of ITRF2000 to NNR-NUVEL1A does not guarantee that the ITRF2000 frame satisfies an NNR condition that is internally consistent with the surface velocity field implied by the ITRF2000 station velocities. A more accurate NNR condition is one based on an NNR model that is derived from our best knowledge of the present-day horizontal surface velocity field everywhere on the Earth's surface. Such models are starting to emerge through a combination of geodetic velocity data and interpolation and/or finite element techniques [*Kreemer et al.*, 2000; *Drewes and Angermann*, 2001]. One such model is the Global Strain Rate Map (GSRM) [*Kreemer et al.*, 2003], which is parameterized as a set of rigid spherical caps with deformable plate boundary zones between them. GSRM is mainly based on geodetic velocity estimates and is defined in a self-consistent manner by the rigid body rotations of 25 spherical caps and a velocity gradient tensor field for the plate boundary zones [*Kreemer et al.*, 2003]. When using the GSRM model, the NNR model is implicitly derived from a plate-fixed kinematic model. This study aims to quantify the stability and sensitivity of the latest GSRM-NNR frame in terms of modeling assumptions and data input. These tests are necessary to verify the stability of the GSRM-NNR model and to assess its difference with ITRF. This, in turn, would be important if a model like GSRM-NNR-2 were to be adopted as the NNR model for the alignment of future generations of ITRF.

## 2. Kinematic Model

[4] We use a core velocity solution onto which available published velocities are transformed. The core solution consists of a velocity field estimated from weekly global and regional GPS solutions from the International GNSS Service (IGS) analysis for 372 sites between 1996.75 and 2005.5. Velocity solutions are computed for four IGS

[1]Nevada Bureau of Mines and Geology, and Seismological Laboratory, University of Nevada, Reno, Nevada, USA.
[2]School of Civil Engineering and Geosciences, Newcastle University, Newcastle upon Tyne, UK.
[3]Also at School of Civil Engineering and Geosciences, Newcastle University, Newcastle upon Tyne, UK.
[4]Department of Geosciences, State University of New York, Stony Brook, New York, USA.


0094-8276/06/2006GL027058$05.00

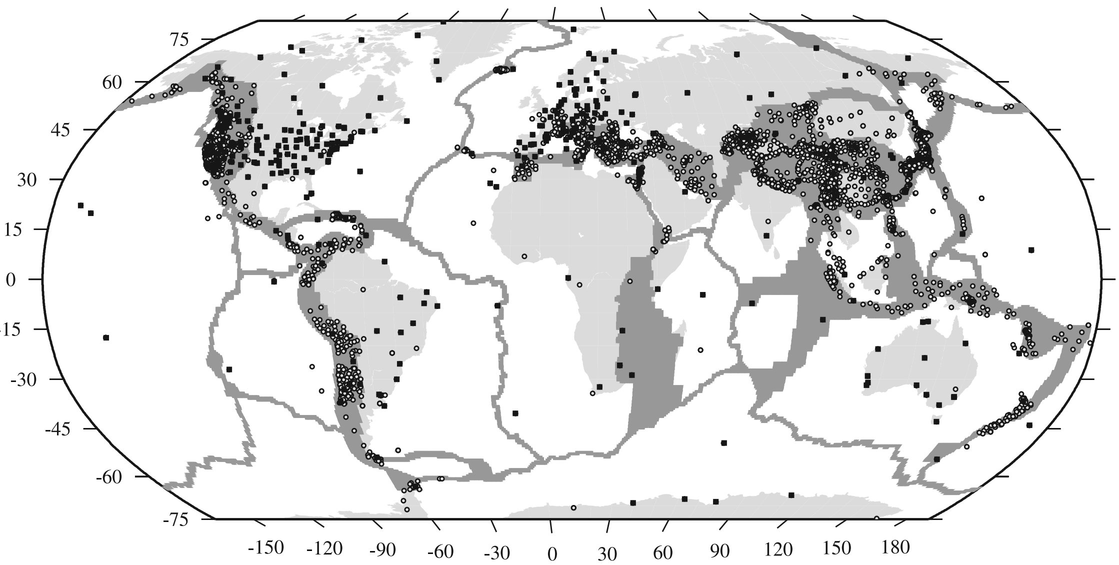


**Figure 1.** Grey shaded zones outline the extent of the plate boundary zones assumed in this study. Black squares are sites of our core solution and open circles are locations of all other velocities incorporated to estimate the NNR frame.

regional associate analysis centers (Australia, Europe, South and North America) and are attached to a central solution computed from re-processed results from the IGS analysis center at Scripps Institute of Oceanography. Using a free-network approach [*Davies and Blewitt*, 2000] all stations with a minimum of 104 observations over a minimum of 2.5-year data-span are fitted to a constant linear station motion model. The minimum data requirements are introduced so that velocity estimates are reliable in the presence of seasonal signals [*Blewitt and Lavallée*, 2002]. The resulting free network solution is aligned to ITRF2000 by estimating a 14 parameter Helmert transformation.

[5] Station velocity solutions from 93 published (or otherwise available) studies are aligned to the core solution through a 6-parameter Helmert transformation (rotation and translation rate) using horizontal velocities at collocated sites. (All solutions are based on the GPS technique, except for the global Very Long Baseline Interferometry (VLBI) solution (NASA Goddard Space Flight Center VLBI Group, Solution 2004en, 2004, data products available electronically at http://lupus.gsfc.nasa.gov/global).) If a translation rate in addition to a rotation rate does not significantly improve the fit (as defined through an F-test statistics) only a rotation rate is applied as part of the transformation. This process is iterative (and non-unique) because for some station velocity solutions a sufficient number of collocated sites only occurs once a number of other station velocity solutions have been attached to the core solution. A few station velocity solutions remain with insufficient collocated sites, and those velocities are rotated in the core solution frame (i.e., ITRF2000) in the process of solving for the global velocity gradient tensor field [*Kreemer et al.*, 2003]. All transformation results and references to the incorporated station velocity solutions are tabulated in the auxiliary material[1]. The current database consists of 5732 velocities at 5459 sites (Figure 1). Unlike the model presented by *Kreemer et al.* [2003] we do not include in this study Quaternary fault slip rate data in central Asia. We exclude fault data in this study, because 1) since the earlier GSRM models the amount of geodetic velocities has increased tremendously in central Asia, eliminating the need for additional geologic data to constrain the velocity gradient field there, and 2) even though fault data may help to localize strain rates near faults, such information rarely alters the local velocity gradient (let alone the global integral of velocity crossed with radial vector) in a significant way.

[6] For all plates with at least two velocities we calculate an angular velocity in ITRF2000 (Table 1). We then convert these estimates into relative angular velocities with respect to the Pacific plate and apply the results as plate boundary velocity constraints while inverting for the velocity gradient tensor field for the plate boundary zones. We apply PA-fixed geologically-inferred angular velocities to those plates that do not have sufficient geodetic coverage. These angular velocities are obtained by combining geologic rates with geodetic relative angular velocities obtained in this study (Table 2).

[7] We satisfy (1) by following *Kreemer and Holt* [2001], which will yield the NNR pole for the reference plate and we then subsequently calculate the NNR angular velocities for all plates (Table 1) using the relative angular velocities. The difference between our NNR frame and ITRF2000 is taken as the difference between our PA-ITRF2000 and PA-NNR angular velocities, and expressed as an ITRF2000 relative to NNR (e.g., ITRF2000-NNR) angular velocity (Table 3).

## 3. Testing Alternative Models

[8] We now test several variations to our data input and model assumptions and we assess their effect on the global velocity integral, and thus the NNR frame.

[9] 1. In this case we only use our core solution of 372 velocities and do not attach any other study. Consequently,

[1]Auxiliary materials are available at ftp://ftp.agu.org/apend/gl/2006gl027058.

**Table 1.** Plate Angular Velocities[a]

| Plate | N[b] | ITRF2000 | | | | | | No-Net-Rotation | | |
|---|---|---|---|---|---|---|---|---|---|---|
| | | $\omega_x$, ° Myr$^{-1}$ | $\omega_y$, ° Myr$^{-1}$ | $\omega_z$, ° Myr$^{-1}$ | ρ(x, y) | ρ(x, z) | ρ(y, z) | $\omega_x$ | $\omega_y$ | $\omega_z$ |
| Amur | 38 | −0.063 ± 0.006 | −0.118 ± 0.009 | 0.248 ± 0.012 | −0.88 | −0.89 | 0.95 | −0.055 | −0.130 | 0.266 |
| Anatolia | 3 | 0.907 ± 0.180 | 0.460 ± 0.122 | 0.891 ± 0.170 | 1.00 | 1.00 | 1.00 | 0.915 | 0.448 | 0.910 |
| Antarctica | 12 | −0.065 ± 0.001 | −0.087 ± 0.001 | 0.186 ± 0.003 | 0.14 | −0.18 | 0.38 | −0.057 | −0.099 | 0.205 |
| Arabia | 9 | 0.325 ± 0.014 | −0.001 ± 0.016 | 0.417 ± 0.011 | 0.98 | 0.96 | 0.96 | 0.334 | −0.013 | 0.436 |
| Australia | 36 | 0.414 ± 0.002 | 0.314 ± 0.001 | 0.328 ± 0.001 | −0.71 | 0.71 | −0.60 | 0.422 | 0.302 | 0.347 |
| Capricorn[c] | – | – | – | – | – | – | – | 0.422 | 0.318 | 0.409 |
| Caribbean | 5 | −0.016 ± 0.006 | −0.207 ± 0.015 | 0.161 ± 0.006 | −0.93 | 0.74 | −0.78 | −0.008 | −0.219 | 0.180 |
| Caroline[c] | – | – | – | – | – | – | – | 0.462 | −0.132 | −0.747 |
| Cocos[c] | – | – | – | – | – | – | – | −0.617 | −1.211 | 0.648 |
| Eurasia | 157 | −0.030 ± 0.001 | −0.137 ± 4e-4 | 0.208 ± 0.001 | 0.29 | 0.93 | 0.33 | −0.022 | −0.149 | 0.226 |
| India | 5 | 0.298 ± 0.011 | −0.028 ± 0.049 | 0.389 ± 0.015 | 0.95 | 0.88 | 0.92 | 0.307 | −0.041 | 0.408 |
| J. de Fuca[c] | – | – | – | – | – | – | – | 0.577 | 0.890 | −0.859 |
| Nazca | 5 | −0.076 ± 0.004 | −0.408 ± 0.012 | 0.436 ± 0.006 | 0.14 | 0.08 | 0.68 | −0.068 | −0.420 | 0.454 |
| N. America | 104 | 0.022 ± 4e-4 | −0.193 ± 0.002 | −0.017 ± 0.002 | −0.18 | 0.16 | −0.76 | 0.030 | −0.205 | 0.002 |
| Nubia | 11 | 0.032 ± 0.003 | −0.159 ± 0.001 | 0.200 ± 0.001 | −0.07 | 0.30 | −0.08 | 0.040 | −0.172 | 0.218 |
| Okhotsk | 6 | 0.151 ± 0.161 | −0.228 ± 0.064 | −0.231 ± 0.259 | −0.99 | −1.00 | 1.00 | 0.159 | −0.241 | −0.213 |
| Pacific | 30 | −0.098 ± 0.002 | 0.281 ± 0.002 | −0.608 ± 0.001 | 0.25 | 0.08 | −0.06 | −0.090 | 0.269 | −0.589 |
| Philip. Sea | 3 | 0.483 ± 0.206 | −0.216 ± 0.225 | −0.652 ± 0.125 | −0.98 | −0.99 | 0.99 | 0.491 | −0.229 | −0.634 |
| Rivera[c] | – | – | – | – | – | – | – | −1.232 | −4.054 | 1.582 |
| Scotia[c] | 1 | – | – | – | – | – | – | −0.011 | −0.148 | −0.008 |
| Somalia | 7 | −0.010 ± 0.008 | −0.199 ± 0.008 | 0.253 ± 0.003 | 0.91 | 0.11 | 0.10 | −0.002 | −0.211 | 0.272 |
| S. America | 37 | −0.055 ± 0.002 | −0.085 ± 0.002 | −0.047 ± 0.002 | −0.77 | −0.69 | 0.76 | −0.047 | −0.098 | −0.029 |
| S. China | 24 | −0.078 ± 0.012 | −0.107 ± 0.028 | 0.293 ± 0.016 | −0.98 | −0.97 | 0.98 | −0.070 | −0.120 | 0.312 |
| Sunda | 21 | −0.002 ± 0.006 | −0.265 ± 0.021 | 0.252 ± 0.004 | −0.92 | −0.46 | 0.49 | 0.006 | −0.277 | 0.270 |
| Tarim | 5 | −0.003 ± 0.010 | −0.528 ± 0.116 | −0.110 ± 0.096 | 0.90 | 0.90 | 1.00 | 0.005 | −0.540 | −0.091 |

[a]ρ(x, y), ρ(x, z), and ρ(y, z) are the correlation coefficient between x and y, x and z, and y and z directions, respectively.
[b]Number of velocities per plate.
[c]These plates have insufficient velocities to determine their angular velocity geodetically. Their no-net-rotation angular velocity is inferred from including published geologic rates. One could infer their ITRF2000 angular velocities by subtracting our ITRF2000-NNR angular velocity (Table 3).

for many plate boundary zones the site coverage is very small, and for several plates the geographic coverage is more limited (e.g., Pacific, Nazca, Somalia) than our preferred solution (Figure 1) leading to some different plate angular velocities.

[10] 2. Instead of our own core velocity solution we use another global solution (Z. Altamimi, personal communication, 2006) to which to attach the published station velocity solutions. Because Altamimi's solution already has the DORIS and VLBI techniques included, we do not attach velocities from the VLBI technique, as we would otherwise do (see Table S1).

[11] 3. *Kreemer and Holt* [2001] argued that plate boundary zones, which deform, should not be modeled as being part of adjacent rigid plates, and they showed that such a false assumption significantly changed their NNR model. Most plate boundaries are now fairly well covered with geodetic velocity measurements (Figure 1), but any significant future change to the global velocity field could arguably come from a refined knowledge of the velocity field there. As an extreme test we calculate the velocity gradient tensor field without using any data within the plate boundary zones. The velocity field within those zones is therefore simply the velocity gradient field that satisfies the plate velocity constraints imposed on the rigid adjacent plates and blocks.

[12] 4. Our estimate of the angular velocities of some plates (e.g., North America (NA), Eurasia) could change significantly once the effects of glacial isostatic adjustments (GIA) have been properly accounted for. In an ongoing study of NA plate motion the GIA signal has been removed from the observed velocities in order to obtain an improved secular estimate [*Blewitt et al.*, 2005]. As a test we use that estimate ($\omega_x$ = 0.0183, $\omega_y$ = −0.1851, $\omega_z$ = −0.0241), converted to a PA-fixed frame, as a velocity boundary constraint instead of that listed in Table 1.

[13] 5. Some plates' geodetic motions are currently undetermined because there are insufficient geodetic velocities to calculate an angular velocity. Examples are the Juan de Fuca (JF) and Cocos (CO) plates. Geologic rates have been estimated for these plates (Table 2), but it is possible that these are significantly different than the actual present-day rates. For example, such a discrepancy has been found for the Nazca plate [*Angermann et al.*, 1999; *Norabuena et al.*, 1999], which geodetic rotation rate relative to South America is 84% of that of NUVEL-1A [*Kreemer et al.*, 2003]. As a test we impose an angular velocity constraint for the unconstrained plates (JF, CO, Rivera, Scotia, Cap-

**Table 2.** Angular Velocities of Plates That Are Not Constrained by Geodetic Velocities[a]

| Plate | Lat., °N | Lon., °E | $\dot{\omega}$, °Myr$^{-1}$ | Study |
|---|---|---|---|---|
| Capricorn | 62.8 | 5.5 | 1.12 | *DeMets et al.* [2005] |
| Caroline | −13.0 | −36.0 | 0.70 | *Weissel and Anderson* [1978] |
| Cocos | 38.2 | −109.6 | 2.00 | *DeMets* [2001] |
| J. de Fuca | −16.5 | 43.0 | 0.95 | *Wilson* [1993] |
| Rivera | 25.9 | −104.8 | 4.97 | *DeMets and Wilson* [1997] |
| Scotia | 53.9 | −79.3 | 0.72 | *Thomas et al.* [2003] |

[a]Angular velocities are with respect to the Pacific plate. If study provided an angular velocity with respect to a plate other than Pacific, we have added to the published values the appropriate relative angular velocity determined geodetically in this study.

**Table 3.** ITRF2000-NNR Angular Velocities[a]

| | $\omega_x$ | $\omega_y$ | $\omega_z$ | $v_{max}$ | $u_{max}$ |
|---|---|---|---|---|---|
| Pref. Model | 0.00811 | −0.01222 | 0.01860 | 2.6 | – |
| Case 1 | 0.01641 | −0.01860 | 0.02300 | 4.3 | 1.8 |
| Case 2 | 0.01124 | −0.01087 | 0.01744 | 2.6 | 0.6 |
| Case 3 | 0.00759 | −0.01485 | 0.01950 | 2.9 | 0.3 |
| Case 4 | 0.00854 | −0.01272 | 0.01868 | 2.7 | 0.1 |
| Case 5 | 0.00960 | −0.01185 | 0.02367 | 3.1 | 0.6 |
| Case 6 | 0.00896 | −0.01239 | 0.01982 | 2.8 | 1.8 |

[a]Difference between our NNR model and ITRF2000 expressed as an angular velocity (° $Myr^{-1}$) and $v_{max}$ (mm $yr^{-1}$) which is the horizontal velocity 90° away from corresponding Euler pole. Different cases are discussed in text. $u_{max}$ is the maximum velocity difference corresponding to the relative angular velocity between our preferred NNR model and the different cases.

ricorn, Caroline) that is also at 84% of the rate presented in the literature.

[14] 6. Any real net translation rate of the crust relative to the Earth's center of mass that is not due to tectonic deformation is likely to be small, <1mm $yr^{-1}$ [*Trupin et al.*, 1992; *Argus et al.*, 1999; *Greff-Lefftz*, 2000]. Geodesy has not yet reached the required precision to quantify any such translation rate; furthermore, defining the translation rate of the frame origin is confounded by orbit errors and deficiencies in tracking network sampling [*Argus et al.*, 1999]. *Altamimi et al.* [2002] found that SLR translation rates can be ~1.0 mm $yr^{-1}$ (in Z-direction) and can be even larger for GPS. The ITRF origin rate definition is therefore uncertain at this level.

[15] To test the affect on the NNR frame, we translate our velocity solution with 1.7 mm $yr^{-1}$ towards 36°N and 111°E, which changes the horizontal velocity field, before we calculate plate angular rotations and determine the NNR frame. This translation rate is equal to that inferred on the basis of the comparison between vertical VLBI velocities and GIA predictions [*Argus*, 1996]. Although this translation rate does not necessarily reflect any existing translation rate bias in ITRF2000, it serves as an illustration. It should be noted that the direction of the translation rate is important, because different directions will impact the plate angular velocities differently, and therefore the impact on the NNR frame will vary with the direction of any translation rate.

## 4. Discussion and Conclusions

[16] We find that the inter-model differences between most of our different NNR model realizations are relatively small. The difference between the NNR models in Table 3 leads to a maximum velocity (at 90° away from the Euler pole corresponding to the relative angular velocities: $u_{max}$) that is 1.8 mm $yr^{-1}$ for Case 1, 1.8 mm $yr^{-1}$ for Case 6, and ≤0.6 mm $yr^{-1}$ for the other cases. It is anticipated that the difference between Case 1 and our preferred model will diminish in the future as the spatial coverage of the IGS network (and hence our core solution) increases. The incorporation of a large translation rate of 1.7 mm $yr^{-1}$ results in the largest difference in NNR frame compared to our preferred model. The fact that the difference between the ITRF2000-NNR angular velocities for Case 6 and our preferred model (Table 3) is minimal is because the additional translation rate in Case 6 equally affects the ITRF and NNR velocities. We conclude that the assessment of a possible frame translation rate bias should be a subject for continuing research, because it not only affects the origin definition but, if the bias is significant, the NNR frame as well. Also, future work needs to assess the sensitivity of the direction of the translation rate bias on the NNR frame.

[17] Our results indicate that if we use the SNARF angular velocity for North America instead of the one based on velocities that are not adjusted for the effects of GIA, our NNR frame is not significantly affected. However, it is not certain whether this conclusion still stands if SNARF-like angular velocities would be available, and used, for other plates, such as Eurasia.

[18] *Kreemer and Holt* [2001] showed that it is important to not model the plate boundary zones as if they are part of the rigid adjacent plates. That conclusion still stands, but the small difference between Case 3 and our preferred model indicates that the NNR frame is not very sensitive to the fine details of the velocity field within the plate boundary zones (the difference in models relates to a maximum differential velocity of 0.3 mm $yr^{-1}$). When we set the rates for the unconstrained plates to be 84% of the most recent estimated geologic rates (i.e., Case 5) the difference in NNR model is relatively small. In our preferred model the summed areal velocity of the six unconstrained plates is 2.6% of the global integral, and evidently changing those velocities has no significant effect on the outcome of (1). However, further tests show that if we change those plate rates to being 50% of published geologic rates the impact on NNR is significant. Such a drastic difference between true and inferred geologic rates is, on the other hand, probably unrealistic.

[19] The difference between our various NNR model cases is small compared to the difference between any of our NNR frames and ITRF2000. For most cases the difference amounts to a rotation whose associated Euler pole can generally be found in western Canada. The related velocity difference can be up to 2.6–3.1 mm $yr^{-1}$ ($v_{max}$: Table 3) in parts of Eurasia, South America, Africa and the Pacific (not considering Case 1). This is a large difference considering the uncertainty in the NNR frame and the standard velocity error for most (continuous) stations. The difference is slightly larger than the 2.3 mm $yr^{-1}$ that *Altamimi et al.* [2003] estimated to be the maximum velocity related to the difference between ITRF2000 and the NNR model of *Kreemer and Holt* [2001] (as estimated using the velocities at 50 ITRF core sites). We conclude that ITRF2000 does not satisfy the NNR constraint if the NNR model is based on the actual present-day velocity of the entire Earth's surface.

[20] For matters of consistency it would be acceptable for future ITRF generations to continue having the frame aligned to the NNR-NUVEL1A model, even if that entails that ITRF does not satisfy a true NNR condition based on present-day surface kinematics. However, one of the main problems with the current alignment procedure is that it is limited to using only sites far away from plate boundaries. The use of the GSRM-NNR-2 model instead of NNR-NUVEL1A would alleviate that restriction and would simultaneously ensure a proper NNR condition for ITRF. We show here that given a small frame translation rate bias and sufficient global coverage, GSRM-NNR-2 has sub mm $yr^{-1}$

stability. Whether it is worth making the change from using NNR- NUVEL1A to a model like GSRM-NNR (and such change may also require significant change in Earth Orientation Parameters) should remain subject to ongoing research and discussions.

[21] **Acknowledgments.** We thank the IGS community for both GPS data and SINEX products, in particular we thank the IGS analysis centers; Australian Surveying and Land Information Group (AUSLIG), European Coordinating Regional Network Analysis Center (EUREF), Natural Resources Canada (NRCAN), Scripps Institute of Oceanography (SIO) and the IGS regional network for South America (SIRGAS) for providing weekly SINEX. We thank Z. Altamimi for making his most recent velocity data set available to us. This research has made use of NASA Goddard Space Flight Center's VLBI terrestrial reference frame solution number 2004en. We thank the following individuals for kindly providing us with (supplemental) geodetic velocities from their studies: T. Árnadóttir, A. Avallone, J. Beavan, B. Brooks, E. Calais, C. DeMets, R. Fernandez, J. Freymueller, B. Hager, W. Hammond, T. Kato, J. Klotz, P. LaFemina, S. Mazzotti, S. McClusky, J.-M. Nocquet, J. Oldow, C. Reigber, T. Sagiya, R. Trenkamp (and INGEOMINAS), R. Smalley, R. Smith. A. Socquet, P. Tregoning, and A. van der Hoeven. We are grateful to the Jet Propulsion Laboratory for the GIPSY OASIS II software and precise GPS orbit products. This work has been conducted with support from NASA's Solid Earth and Natural Hazards grant SENH-0225-0008 and a Royal Society University Research Fellowship to DAL. This paper benefited from comments by Z. Altamimi and an anonymous reviewer.

## References

Altamimi, Z., P. Sillard, and C. Boucher (2002), ITRF2000: A new release of the International Terrestrial Reference Frame for earth science applications, *J. Geophys. Res.*, *107*(B10), 2214, doi:10.1029/2001JB000561.

Altamimi, Z., P. Sillard, and C. Boucher (2003), The impact of a No-Net-Rotation Condition on ITRF2000, *Geophys. Res. Lett.*, *30*(2), 1064, doi:10.1029/2002GL016279.

Angermann, D., et al. (1999), Space-geodetic estimation of the Nazca-South America Euler vector, *Earth Planet. Sci. Lett.*, *171*, 329–334.

Argus, D. F. (1996), Postglacial rebound from VLBI geodesy: On establishing vertical reference, *Geophys. Res. Lett.*, *23*, 973–976.

Argus, D. F., and R. G. Gordon (1991), No-net-rotation model of current plate velocities incorporating plate motion model NUVEL-1, *Geophys. Res. Lett.*, *18*, 2039–2042.

Argus, D. F., et al. (1999), Glacial isostatic adjustment observed using very long baseline interferometry and satellite laser ranging geodesy, *J. Geophys. Res.*, *104*, 29,077–29,093.

Blewitt, G., and D. Lavallée (2002), Effect of annual signals on geodetic velocity, *J. Geophys. Res.*, *107*(B7), 2145, doi:10.1029/2001JB000570.

Blewitt, G., et al. (2005), A stable North America reference frame (SNARF): First release, paper presented at UNAVCO-IRIS Joint Workshop, Stevenson, Wash.

Davies, P., and G. Blewitt (2000), Methodology for global geodetic time series estimation: A new tool for geodynamics J, *Geophys. Res.*, *105*, 11,083–11,100.

DeMets, C. (2001), A new estimate for present-day Cocos-Caribbean plate motion: Implications for slip along the Central American volcanic arc, *Geophys. Res. Lett.*, *28*, 4043–4046.

DeMets, C., and D. Wilson (1997), Relative motions of the Pacific, Rivera, North American, and Cocos plates since 0.78 Ma, *J. Geophys. Res.*, *102*, 2789–2806.

DeMets, C., et al. (1994), Effect of recent revisions to the geomagnetic reversal time-scale on estimates of current plate motions, *Geophys. Res. Lett.*, *21*, 2191–2194.

DeMets, C., et al. (2005), Motion between the Indian, Capricorn and Somalian plates since 20 Ma: Implications for the timing and magnitude of distributed lithospheric deformation in the equatorial Indian ocean, *Geophys. J. Int.*, *161*, 445–468.

Drewes, H., and D. Angermann (2001), The actual plate kinematic and crustal deformation model 2000 (APKIM2000) as a geodetic reference system, paper presented at IAG Scientific Assembly, Int. Assoc. of Geod., Budapest.

Greff-Lefftz, M. (2000), Secular variation of the geocenter, *J. Geophys. Res.*, *105*, 25,685–625,692.

Kreemer, C., and W. E. Holt (2001), A no-net-rotation model of present-day surface motions, *Geophys. Res. Lett.*, *28*, 4407–4410.

Kreemer, C., et al. (2000), On the determination of a global strain rate model, *Earth Planets Space*, *52*, 765–770.

Kreemer, C., et al. (2003), An integrated global model of present-day plate motions and plate boundary deformation, *Geophys. J. Int.*, *154*, 8–34.

McCarthy, D. M., and G. Petit (2004), *IERS Conventions, 2003*, *IERS Tech. Note 32*, 127 pp., Verlag des Bundesamts für Kartogr. und Geod., Frankfurt, Germany.

Norabuena, E. O., et al. (1999), Decelerating Nazca-South America and Nazca-Pacific plate motions, *Geophys. Res. Lett.*, *26*, 3405–3408.

Sella, G. F., T. H. Dixon, and A. Mao (2002), REVEL: A model for Recent plate velocities from space geodesy, *J. Geophys. Res.*, *107*(B4), 2081, doi:10.1029/2000JB000033.

Solomon, S. C., and N. H. Sleep (1974), Some physical models for absolute plate motions, *J. Geophys. Res.*, *79*, 2557–2567.

Thomas, C., et al. (2003), Motion of the Scotia Sea plates, *Geophys. J. Int.*, *155*, 789–804.

Trupin, A. S., et al. (1992), Effect of melting glaciers on the Earths rotation and gravitational field—1965–1984, *Geophys. J. Int.*, *108*, 1–15.

Weissel, J. K., and R. N. Anderson (1978), Is there a caroline plate?, *Earth Planet. Sci. Lett.*, *41*, 142–158.

Wilson, D. S. (1993), Confidence intervals for motion and deformation of the Juan de Fuca plate, *J. Geophys. Res.*, *98*, 16,053–16,071.

G. Blewitt and C. Kreemer, Nevada Bureau of Mines and Geology, and Seismological Laboratory, University of Nevada, Reno, NV 89557, USA. (kreemer@unr.edu)

W. E. Holt, Department of Geosciences, State University of New York, Stony Brook, NY 11790, USA.

D. A. Lavallée, School of Civil Engineering and Geosciences, Newcastle University, Newcastle upon Tyne, NE1 7RU, UK.